DYNAMICS OF A SOLAR SAIL NEAR A HALO ORBIT

A. Farrés[a,*], À. Jorba[a]

[a] *Departament de Matemàtica Aplicada i Anàlisi, Univeritat de Barcelona Gran Via de les Corts Catalanes 585, 08007 Barcelona, Spain*

Abstract

In this work we are interested in the local dynamics around a Halo - type orbit for a solar sail and how it varies when the sail orientation changes. To model the dynamics of a solar sail we have considered the Restricted Three Body Problem adding the solar radiation pressure (RTBPS). We know that the RTBPS has a 2D family of equilibrium points parametrised by the two angles that define the sail orientation. First we will describe the families of periodic and quasi-periodic orbits that appear around the different equilibrium points. We will find planar, vertical and Halo - type orbits around the different equilibria. Finally, we will focus on a Halo - type orbit and describe the natural dynamics around it. We will discuss the possibility of using this knowledge to derive station keeping strategies for a solar sail.

Keywords: Periodic orbits, Station keeping, Centre manifold, Invariant manifolds, Low - thrust

1. Introduction

Solar Sailing is a proposed form of spacecraft propulsion using large membrane mirrors. The impact of the photons emitted by the Sun on the surface of the sail and their further reflection produce momentum on it. Although the acceleration produced by this reflection is smaller than the one achieved by a 'traditional' spacecraft it is continuous and unlimited. This makes long term missions more accessible (18) and opens a wide new range of possible mission applications that cannot be achieved by a traditional spacecraft, e.g. Geostorm Warning Mission (16; 26; 1) and Polar Observer (16).

The acceleration given by the sail depends on the orientation of the sail and its efficiency. The sail orientation is parametrised by two angles α and δ and the sail efficiency is given in terms of the sail lightness number β. In this paper we consider the sail to be flat and perfectly reflecting, so the force due to the solar radiation pressure is normal to the surface of the sail. We have taken the Sun - Earth Restricted Three Body Problem (RTBP) and added the solar radiation pressure as a model.

If the radiation pressure is discarded, it is well known that the RTBP has five equilibrium points $L_{1,\dots,5}$, three of them are linearly unstable and are placed on the axis joining the two primaries. Around these fixed points, there are two families of unstable periodic orbits, the vertical and horizontal Lyapunov families, and a set of invariant tori. For a certain energy level the well known family of Halo orbits appears.

When we add the solar radiation pressure, these five equilibrium points $L_{1,\dots,5}$ are replaced by a 2D surface of equilibria parametrised by the two angles defining the sail orientation (18; 1) . Around some of these equilibrium points we also find families of periodic orbits and invariant tori.

For the particular case of $\alpha = 0$ (i.e. we just allow the sail orientation to vary vertically w.r.t. the Sun - sail line direction) the system is time reversible.

*corresponding author

Email addresses: ari@maia.ub.es (A. Farrés), angel@maia.ub.es (À. Jorba)

Now the system has five 1D families of equilibria parametrised by δ. The reversible character (21; 13) of the system ensures us, that under certain constraints on these equilibrium points, there will exist families of periodic and quasi-periodic orbits around them (8). In section 2 we will describe these families of equilibrium points and show where there is periodic and quasi-periodic motion. Then we will describe the phases space portrait for different sail orientations. We will see that there are families of planar and vertical periodic orbits, as well as Halo - type orbits around the different equilibrium points.

When $\alpha \neq 0$ the linear dynamics around the equilibrium points, in most cases, contains a cross product with a source or a sink. A detailed study on the non-linear dynamics around them should be done to see if there can exist periodic or quasi-periodic motion around them. This is still work in progress.

Halo orbits have already been used as a target for several mission, such as SOHO, Genesis or more recently the two probes Herschel and Plank. Halo orbits offer an interesting location in the Earth - Sun or Earth - Moon system, that allows a satellite to make observations of space and at the same time maintain communication with the Earth. Nevertheless, these orbits are unstable and a station keeping strategies must be applied to maintain the satellite close to it.

In Section 3 we focus on the family of Halo - type orbits for a solar sail. We will describe the natural dynamics around these families of periodic orbits (i.e. its stable and unstable manifolds) and study how variations on the sail orientation affects them. We want to study if it is possible to find a sequence of changes on the sail orientation to maintain the trajectory of a solar sail close to a Halo - type orbit. The final goal is to follow the ideas described in (6; 5) for the station keeping around an equilibrium point to derive these strategies.

2. Solar Sails on the RTBP

To describe the dynamics of a solar sail in the Earth - Sun system we have taken the RTBP and added the solar radiation pressure (RTBPS). We assume that the Earth and Sun are point masses moving around their common centre of mass in a circular way, and the sail is a massless particle that is affected by the gravitational attraction of both bodies and the solar radiation pressure. We normalise the units of mass, distance and time, so that the total mass of the system is 1, the Sun - Earth distance is 1 and the period of its orbit is 2π. We use a rotating reference system so that Earth and Sun are fixed on the x-axis, z is perpendicular to the ecliptic plane and y defines an orthogonal positive oriented reference system (see Figure 1).

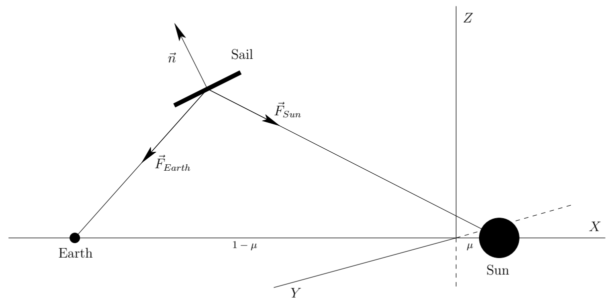

Figure 1: Schematic representation of the position of the two primaries and the solar sail in the synodical reference system.

We have considered the solar sail to be flat and perfectly reflecting, hence the force due to the solar radiation pressure is in the normal direction to the surface of the sail and is given by,

$$\vec{F}_{sail} = \beta \frac{1-\mu}{r_{PS}^2} \langle \vec{r}_s, \vec{n} \rangle^2 \vec{n},$$

where β represents the sail lightness number, $\vec{r}_s$ is the Sun - line direction and $\vec{n}$ is the normal direction to the surface of the sail (both vectors, $\vec{n}$ and $\vec{r}_s$, are normalised).

The sail orientation is parametrised by two angles, α and δ, which allow different definitions (18; 14; 20) . We define them as follows: (i) α is the angle between the projection of the Sun - sail line, $\vec{r}_s$, and the normal vector to the sail, $\vec{n}$, on the ecliptic plane; (ii) δ is the angle between the projection of the Sun - sail line, $\vec{r}_s$, and the normal vector to the sail, $\vec{n}$, on the $y = 0$ plane (see Figure 2).

Finally, using a similar scheme as in (24) , one can see that the equations of motion in the synodical

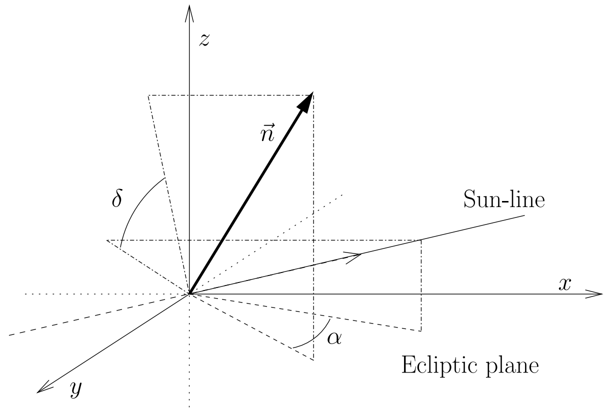

Figure 2: Graphic representation of the two angles (α, δ) that define the sail orientation.

reference system are:

$$
\begin{aligned}
\ddot{X} = \;& 2\dot{Y} + X - \frac{(1-\mu)}{r_{PS}^3}(X-\mu) - \frac{\mu}{r_{PE}^3}(X-\mu+1) \\
& + \beta\frac{(1-\mu)}{r_{PS}^3}\langle \vec{r}_s, \vec{n}\rangle^2 N_X, \\
\ddot{Y} = \;& -2\dot{X} + Y - \left(\frac{(1-\mu)}{r_{PS}^3} + \frac{\mu}{r_{PE}^3}\right)Y \\
& + \beta\frac{(1-\mu)}{r_{PS}^3}\langle \vec{r}_s, \vec{n}\rangle^2 N_Y, \\
\ddot{Z} = \;& -\left(\frac{(1-\mu)}{r_{PS}^3} + \frac{\mu}{r_{PE}^3}\right)Z + \beta\frac{(1-\mu)}{r_{PS}^3}\langle \vec{r}_s, \vec{n}\rangle^2 N_Z,
\end{aligned}
$$

where $r_{PS} = \sqrt{(X-\mu)^2 + Y^2 + Z^2}$ and $r_{PE} = \sqrt{(X-\mu+1)^2 + Y^2 + Z^2}$ are the Sun - sail and Earth - sail distances respectively, $\vec{r}_s = (X-\mu, Y, Z)/r_{PS}$ and $\vec{n} = (N_X, N_Y, N_Z)$.

It is well known (18; 17; 19) that for a fixed value of the sail lightness number (β) this model has a 2D family of equilibrium points parametrised by the two angles that define the sail orientation. Most of these equilibrium points are unstable, but controllable (18). Due to their interesting location, they open a new range of possible mission applications that cannot be achieved by a traditional spacecraft. Two examples are the “Geostorm Warning Mission” (26; 15) and the “Polar Observer” (16). The first one aims to place a sail around a fixed point between the Sun and the Earth, closer to the Sun than L_1 and shifted 5° from the Earth-Sun line. Allowing to make observations of the geomagnetic activity of the Sun and have constant communication with the Earth. The second mission aims to place a sail at a fixed point above the ecliptic plane, being able to constantly observe one of the Earth Poles.

In this work we consider $\beta = 0.051689$, which corresponds to a sail with a characteristic acceleration of $0.3 mm/s^2$ or a sail loading of $30 g/m^2$. This value for the sail lightness number has been considered for the Geostorm Warning Mission (18; 16; 26) and is considered to be a reasonable value for the sail performance of a near term mission. Although the same analysis that we will carry out from now also applies for different values of β.

From now on we will consider the particular case of $\alpha = 0$ and $\delta \in [-\pi/2, \pi/2]$ (i.e. we only allow the sail orientation vary vertically w.r.t. the Sun - sail line direction). Now the system is time reversible by the symmetry

$$R : (t, X, Y, Z, \dot{X}, \dot{Y}, \dot{Z}) \rightarrow (-t, X, -Y, Z, -\dot{X}, \dot{Y}, -\dot{Z}).$$

Reversible systems, under certain constraints, behave locally like Hamiltonian systems (21; 13) . Families of periodic orbits and invariant tori can be found. This is the case of the RTBPS for $\alpha = 0$. When $\alpha \neq 0$ the system is no longer time reversible, and further studies on the dynamics around the equilibrium points must be done.

2.1. Family of equilibrium points

For $\alpha = 0$ the system has five 1D families of equilibria parametrised by δ. Each one is related to one of the classical Lagrangian equilibrium points ($L_{1,\dots,5}$) from the RTBP and the points in each family share similar dynamical properties, we call each family $FL_{1,\dots,5}$. All the equilibrium points in the families $FL_{1,2,3}$ lay on the $Y = 0$ plane and their spectrum are of the form $\{\pm\lambda, \pm \mathrm{i}\omega_1, \pm \mathrm{i}\omega_2\}$. In Figure 3 we see these three families for different values of the sail lightness number β.

The other two families $FL_{4,5}$ do not lay on the $Y = 0$ plane, but are symmetric to each other w.r.t. $Y = 0$. All of these fixed points have a mild instability, and the spectrum of these equilibrium points are of the form $\{\gamma_1 \pm \mathrm{i}\omega_1, \gamma_2 \pm \mathrm{i}\omega_2, \gamma_3 \pm \mathrm{i}\omega_3\}$, where $\gamma_i \neq 0$ but small in absolute value.

The reversible character of the system ensures the existence of periodic and quasi-periodic motion

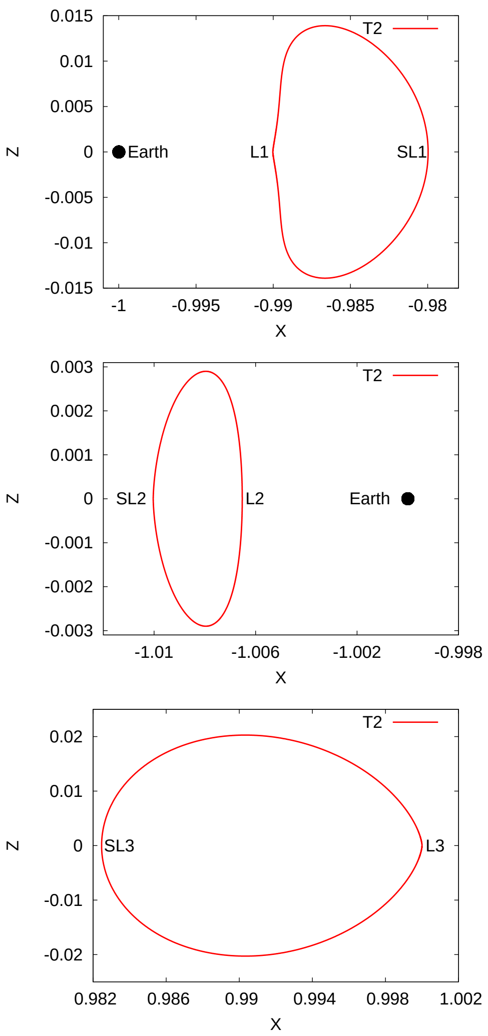

Figure 3: Position of the fixed points for $\beta = 0.051689$. From top to bottom the FL_1, FL_2 and FL_3 families of equilibria.

around the equilibrium points on the $FL_{1,2,3}$ families (21; 13). Notice that for the particular cases $\delta = 0$ and $\delta = \pm\pi/2$ the system is also Hamiltonian. These two cases correspond to: having the sail perpendicular to the Sun - line direction ($\delta = 0$) or neglecting the effect of the sail by aligning it with the Sun - sail line ($\delta = \pm\pi/2$).

2.2. *Non-linear dynamics around equilibria*

From now on we focus on the equilibrium points on the FL_1 family for δ close to zero. These equilibrium points are placed around the $Z = 0$ plane and displaced towards the Sun w.r.t. classical Lagrangian point L_1. We will consider the sail orientation to be fixed along time.

We will show the periodic and quasi-periodic motion around these equilibrium points for different sail orientations. We will describe the variation of the phase space properties when we consider different sail orientations.

As we have mentioned, the RTBPS for $\alpha = 0$ is time reversible. Hence, under certain constraint, these kind of systems behave locally as a Hamiltonian systems (21; 13). The Devaney - Lyapunov's Centre Theorem (4) assures us that under non - resonant conditions between ω_1 and ω_2 there are two families of periodic orbits that emanate from each of the fixed points on FL_1, FL_2 and FL_3.

Now we will show the two families of periodic orbits that emanate from the different equilibrium points on FL_1 and discuss their stability. Moreover, by performing the reduction to the centre manifold around the equilibrium points, we give a complete description of the periodic and quasi - periodic dynamics around them. For a more detailed analysis see (8) .

2.2.1. *Periodic Motion*

As we have already mentioned, for a fixed sail orientation, around the corresponding equilibrium point (p_0), there are two families of periodic orbits. We can distinguish these two families by their vertical oscillation. It can be seen that, for small δ, one of the two complex eigendirections has a wider vertical oscillation than the other, we assume this one to be ω_2.

We call the *$\mathcal{P}$-Lyapunov family* to the family of periodic orbits emanating from p_0 related to ω_1 and the *$\mathcal{V}$-Lyapunov family* to the family emanating from p_0 related to ω_2.

We start with $\delta = 0$ (i.e. the sail is perpendicular to the Sun-line) and study the behaviour of the family of periodic orbits. Then we see how they vary when we take a different sail orientation. We will only consider $\delta \geq 0$, as the system is also symmetric by

$$S : (X, Y, Z, \dot{X}, \dot{Y}, \dot{Z}, \delta) \to (X, Y, -Z, \dot{X}, \dot{Y}, \dot{Z}, -\delta).$$

Due to the reversibility character of the system, all these families of periodic orbits are symmetric with respect to $Y = 0$. This can be taken into account to compute numerically these families.

$\mathcal{P}$-Lyapunov family of periodic orbits

When $\delta = 0$, the family of periodic orbits emanating from p_0 is totally contained on the $Z = 0$ plane. And the orbits have one hyperbolic and one elliptic direction. At a certain point, a pitchfork bifurcation takes place, and two new periodic orbits are born. They are commonly known as Halo orbits.

In Figure 4 we see the continuation scheme for $\delta = 0$. On the horizontal axis we have the continuation parameter (τ) and on the vertical axis the Z component of the point of the orbit on the Poincaré section ($\Sigma = \{Y = 0, \dot{Y} > 0\}$). The points in blue correspond to periodic orbits with two hyperbolic directions, and the points in red correspond to periodic orbits with one hyperbolic and one elliptic direction.

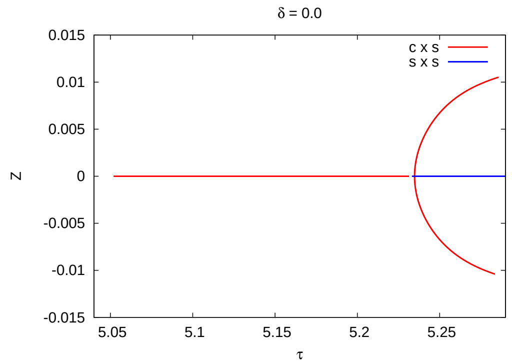

Figure 4: Left: Bifurcations scheme for the continuation of periodic orbits w.r.t τ for the Planar family of periodic orbits for $\delta = 0$.

In Figure 5 we see different projections of these two kinds of periodic orbits.

When $\delta \neq 0$ the family of periodic orbits emanating from the equilibrium point is no longer contained on the $Z = 0$ plane, but for δ small the periodic orbits close to the equilibrium point are almost planar. Moreover, there is no longer a pitchfork bifurcation that gives rise to the two Halo orbits. Now two of the branches have split due to a symmetry breaking (3) on the system for $\delta \neq 0$. Here we have a family of periodic orbits with no change in the stability, although at a certain point the orbits

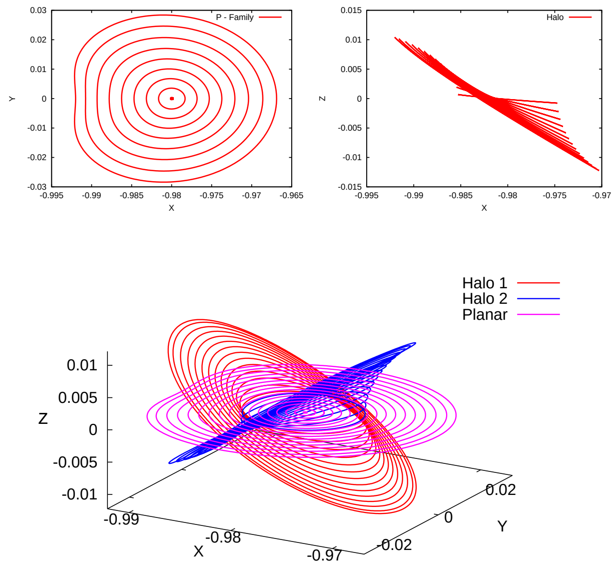

Figure 5: For $\delta = 0$, projections of the planar and Halo family of periodic orbits.

in this family start to gain vertical oscillation, giving rise to Halo - type orbits. Moreover, there are two families of periodic orbits that appear after a saddle - node bifurcation. One of the families is almost planar while the other also has Halo - type orbits.

In Figure 6 we have the same continuation scheme as in Figure 4 for different values of δ, where we can appreciate the symmetry breaking of the pitchfork bifurcations. As before, the points in blue represent periodic orbits with two hyperbolic directions and the ones in red periodic orbits with one hyperbolic and one elliptic direction.

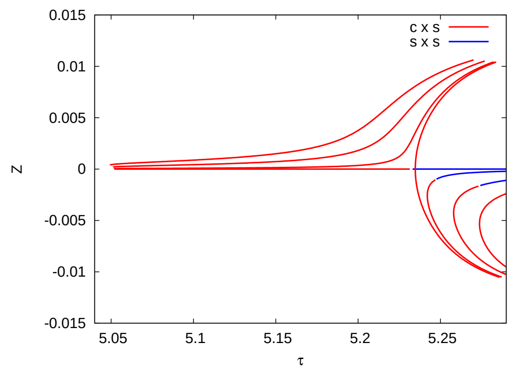

Figure 6: Bifurcation scheme for the continuation of periodic orbits w.r.t. τ for the $\mathcal{P}$-Family of periodic orbits, for $\delta = 0, 0.001, 0.005, 0.01$

In Figure 7 we have different projections of the two families of periodic orbits that we find for $\delta = 0.01$.

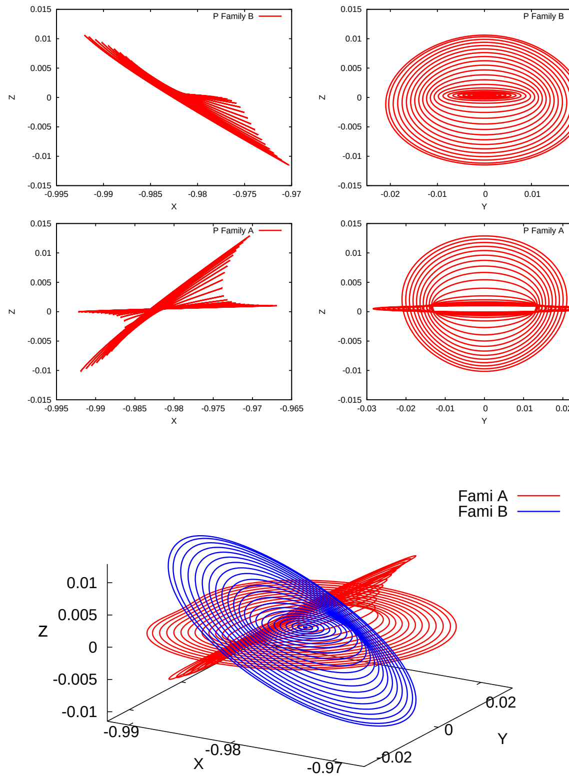

Figure 7: For $\delta = 0.01$, projections of the planar and Halo - type family of periodic orbits.

From the plots on the bottom of Figures 5 and 7 we can see that the qualitative behaviour of the periodic orbits does not differ much for sail orientations with $\alpha = 0$ and $\delta \approx 0$. In these cases we find planar motion and Halo - type orbits.

$\mathcal{V}$ - Lyapunov family of periodic orbits

The orbits in this family cross transversally the planes $Y = 0$ and $Z = Z^*$, where $(X^*, 0, Z^*)$ is the position of the equilibrium point for a given sail orientation (note that $\delta = 0 \Rightarrow Z^* = 0$).

In Figure 8 we can see 3D projections of these families for $\delta = 0, 0.005, 0.01$ and 0.03. Notice that for $\delta = 0$ these orbits have a bow-tie shape symmetric with respect to the $Z = 0$ plane. For $\delta \neq 0$ the periodic orbits on the family that are close to the equilibrium are almost circular, and as we move along

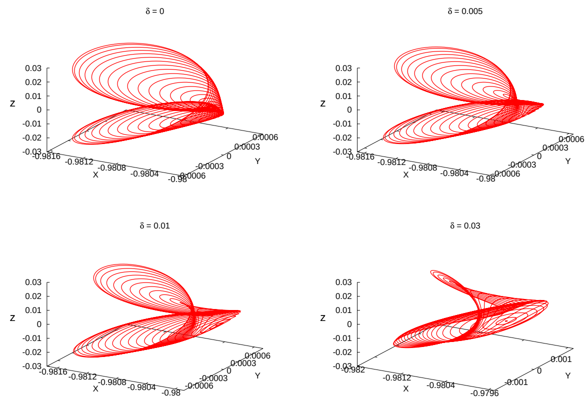

Figure 8: Projections on the X, Y, Z plane of the $\mathcal{V}$ Family of periodic orbits for $\delta = 0, \delta = 0.005, \delta = 0.01$ and $\delta = 0.03$

the family their shape changes taking also a bow-tie shape. Although there is is no longer a symmetry between the two loops.

All of these orbits are unstable, having one hyperbolic and one elliptic direction.

2.2.2. *Quasi Periodic Motion*

As we have said, the linear dynamics of the fixed points on the FL_1 family is the cross product of a saddle and two complex directions with zero real part. Hence, taking arbitrary initial conditions and integrating them numerically to produce plots of the orbits, is not a good option as the trajectories will escape quickly due to the instability produced by the saddle. To get rid of this instability we can performed the so - called reduction to the centre manifold.

We call centre manifold to an invariant manifold that is tangent to the linear subspace generated by the different pairs of complex eigenvectors. This invariant manifold might not be unique, but the Taylor expansion of the graph of this manifold is (2; 22; 25). We can compute a high order approximation of this invariant manifold and restrict the flow on it.

If the system is Hamiltonian we can compute this using a partial normal form scheme of the Hamiltonian (11), but this is not the case, as the system is Hamiltonian only for a small set of parameters. To deal with this situation we can used the graph trans-form method (2; 23) . The idea is to compute, formally, the power expansion of the graph of the centre manifold at the equilibrium point. For further details on these kind of computations see (23; 7) .

For this study we have computed a high order approximation (degree 16) of the graph of the centre manifold around different equilibrium points of the FL_1 family.

Once we have reduced to the centre manifold, we are on a 4D phase space, with (x_1, x_2, x_3, x_4) as the local coordinates on the centre manifold. As a 4D phase space is difficult to visualise, we need to perform suitable Poincaré sections to reduce the phase space dimension.

We have considered the function:

$$
\begin{aligned}
J_C &= (\dot{X}^2 + \dot{Y}^2 + \dot{Z}^2) - 2\Omega(X, Y, Z) \\
&\quad + 2\beta(1-\mu)\frac{Zr_2}{r_{PS}^3}\cos^2\delta\sin^2\delta,
\end{aligned}
$$

which is a first integral of the system for $\delta = 0$, and for $\delta \neq 0$ the value J_c presents small variations (of order 10^{-6} to 10^{-8}) for trajectories close to the equilibrium point. We use this function to slice the phase space, and have a better understanding of the plots. It is also useful to compare the Hamiltonian behaviour with this non - Hamiltonian one.

To visualise the dynamics on the centre manifold, we first take the Poincaré section $x_3 = 0$ and fix J_C to determine x_4. It can be seen that taking $x_3 = 0$ is like taking $Z = Z^*$ and x_4 is related to $\dot{Z}$. Hence, x_1, x_2 is sort of a linear transformation of the $\{x, y\}$ - plane. For each energy level (J_c) we take several initial conditions and compute for each one 500 iterates of the Poincaré map.

In Figure 9 we have the results for $\delta = 0$ and $J_C = -2.895937, -2.895920, -2.895904$ and -2.895889. We can see that for a fixed energy level, the motion on the section is bounded by a planar Lyapunov orbit, which is fully contained on this section. The vertical Lyapunov periodic orbit crosses transversally this section close to the origin, it is seen as a fixed point. For small values of the energy, the coupling between the two frequencies, ω_1 and ω_2, give rise to a family of invariant tori. As the J_C varies, the Planar Lyapunov orbit changes its

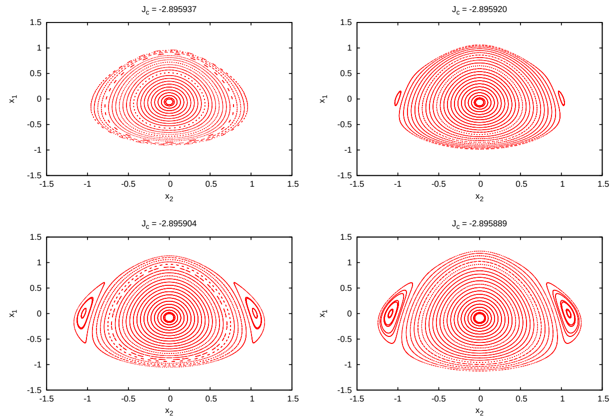

Figure 9: For $\delta = 0$; Poincaré section $x_3 = 0$, the x - axis is x_2 and the y - axis is x_1. From left to right, top to bottom $J_C = -2.895937, -2.895920, -2.895904, -2.895889$.

stability and the two Halo orbits appear. The Halo orbits also cross transversally this section, we see them as the two new fixed points on the section.

We note that the behaviour here is qualitatively the same as for the RTBP close to the collinear points (12). Let us now show how this varies when the sail is no longer perpendicular to the Sun - line (i.e. $\delta \neq 0$).

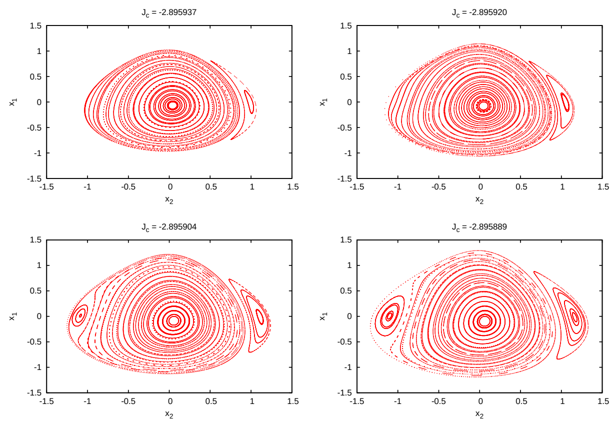

Figure 10: Poincaré section for $x_2 = 0$ taking $\delta = 0.01$. From left to right, top to bottom $\widetilde{J_C} = -2.895937, -2.895920, -2.895904, -2.895889$.

In Figures 10 we have the results for $\delta = 0.01$ for the same values of J_C as before. We see that for small energy levels the coupling between the two frequencies gives rise to families of invariant tori around the equilibrium point, and the central fixed points corresponds to a $\mathcal{V}$-Lyapunov periodic orbit, that crosses transversally this section. As J_C

varies, one Halo orbit appears, seen as the fixed point that appears on the right hand side of the Poincaré sections. If we remember the behaviour of the $\mathcal{P}$-Lyapunov family of periodic orbits for $\delta \neq 0$ seen in the previous section, as we moved along the family, these orbits start to gain Z amplitude, and at some point they cross transversally this section. At some point a saddle - node bifurcation takes place and the other family of Halo - type orbits appears, we see them as a new fixed points on the left hand side of the Poincaré section.

3. Dynamics around a Halo orbit

Halo orbits are placed on a privileged location, that has been already considered for different missions. For instance, the SOHO telescope has been orbiting around a Halo orbit near the Sun - Earth L_1 since 1995, making observation of the Sun's activity. More recently, Herschel and Plank was sent to orbit near two Halo orbits about the Sun - Earth L_2, to make observations of far away galaxies and the deep space.

We will focus on a Halo - type orbit for a solar sail on the RTBPS. Our final goal is to derive station keeping strategies for a solar sail around these orbits. We want to use dynamical system tools to derive such strategies. The key point is to understand the geometry of the phase space close to a Halo orbit and how variations on the sail orientation affect these geometry. Then, try to move the sail in a way that the phase space acts in our favour.

These ideas are based on the previous works by Gomez et al. (10; 9) on the station keeping around a Halo orbits with a "traditional" thruster and by Farrés et al. (5; 6) on the station keeping of a solar sail around an equilibrium point.

As we have seen in the previous section, if the sail is perpendicular to the Sun - line direction, the phase space portrait around SL_1 has the same structure as the RTBP around the collinear point L_1. In both cases we have two families of Halo orbits. We also know that for suitable sail orientations ($\alpha = 0$ and $\delta \approx 0$) these families persist. In this paper, as an example we consider a Halo orbit around SL_1 for a sail oriented perpendicular to the Sun - sail line (i.e. $\alpha = \delta = 0$). But the ideas that we present here are general enough to be applied to the rest of Halo - type orbits in the system.

We will start by describing the linear dynamics around these orbits and discuss how it varies for small variations on the sail orientation. We will describe the effects of these changes on the trajectory of a solar sail close to a given Halo-type orbit. Finally, we will discuss the possibility of deriving station keeping techniques using dynamical system tools.

3.1. Linear dynamics around a Halo orbit

To fix notation, let us consider the equations of motion for the RTBPS to be written in the compact form:

$$\dot{y} = f(y), \quad y \in \mathbb{R}^6. \tag{1}$$

The first step to study the behaviour close to a Halo orbit is done throughout the first order variational equations:

$$\dot{A} = Df(y(t))A, \quad A \in \mathcal{L}(\mathbb{R}^6, \mathbb{R}^6), \tag{2}$$

with $A(0) = Id$.

We denote by ϕ the flow associated to (1) and $\phi_\tau(y_0)$ the image of the point $y_0 \in \mathbb{R}^6$ at $t = 0$ at a time $t = \tau$. The solution $A(\tau)$ of (2) is the differential matrix, $D\phi_\tau(y_0)$, of $\phi_\tau(y_0)$ with respect to the initial condition (y_0).

For $h \in \mathbb{R}^6$, we have

$$\phi_\tau(y_0 + h) = \phi_\tau(y_0) + D\phi_\tau(y_0) \cdot h + O(|h|^2).$$

Therefore, $\phi_\tau(y_0) + A(\tau) \cdot h$ gives a good approximation of $\phi_\tau(y_0 + h)$ provided h small.

If we consider a periodic orbit of period T, the variational matrix after one period, $A(T)$, is called the monodromy matrix associated to the orbit. The study of the eigenvalues and eigenvectors of this matrix gives us the linear dynamics around the periodic orbit.

For the Halo - type orbits that we consider, the eigenvalues $(\lambda_{1,\dots,6})$ of the monodromy matrix satisfy: $\lambda_1 > 1, \lambda_2 < 1$, $\lambda_3 = \bar{\lambda}_4$ are complex with modulus 1 and $\lambda_5 = \lambda_6 = 1$. These three pairs of eigenvalues have the following geometrical meaning:

- The first pair (λ_1, λ_2), verify $\lambda_1 \cdot \lambda_2 = 1$, and are related to the hyperbolic character of the orbit. The value λ_1 is the largest in absolute value, and is related to the eigenvalue $e_1(0)$, which gives the most expanding direction. After one period, a given distance to the nominal orbit in this direction is amplified in a factor of λ_1. Using $D\phi_\tau$ we can get the image of this vector under the variational flow: $e_1(\tau) = D\phi_\tau e_1(0)$. At each point of the orbit, the vector $e_1(\tau)$ together with the vector tangent to the orbit, span a plane that is tangent to the local unstable manifold (W^u_{loc}). In the same way λ_2 and its related eigenvector $e_2(0)$ are related to the stable manifold and $e_2(\tau) = D\phi_\tau e_2(0)$.

- The second couple (λ_3, λ_4) are complex conjugate eigenvalues of modulus 1. Together with the other two eigenvalues equal to 1 describe the central motion around the periodic orbit. The monodromy matrix, restricted to the plane spanned by the real and imaginary parts of the eigenvectors associated to λ_3, λ_4 is a rotation, hence it has the form
$$\begin{pmatrix} \cos\Gamma & -\sin\Gamma \\ \sin\Gamma & \cos\Gamma \end{pmatrix},$$
where Γ is the argument of λ_3.

- The third couple $(\lambda_5, \lambda_6) = (1, 1)$, is associated to the neutral directions (i.e. non-unstable modes). However, there is only one eigenvector of $A(T)$ with eigenvalue 1. This vector is the tangent vector to the orbit, we call it $e_5(0)$. The other eigenvalue is associated to variations of the energy or any other variable which parametrises the family of periodic orbits. The related eigenvector, is chosen orthogonal to $e_5(0)$ in the 2D space associated to the eigenvalue 1, and gives the tangent direction to the family of Halo orbits. The monodromy matrix restricted to this plane has the form
$$\begin{pmatrix} 1 & \varepsilon \\ 0 & 1 \end{pmatrix}.$$
The fact that ε is not zero is due to the variation of the period when the orbit changes along the family.

To sum up, we can state that, in a suitable basis, the monodromy matrix associated to a Halo - type orbit can be written in the form,

$$J = \begin{pmatrix} \begin{array}{cc|} \lambda_1 & \\ & \lambda_2 \\ \hline \end{array} & & 0 \\ & \boxed{\begin{array}{cc} \cos\Gamma & -\sin\Gamma \\ \sin\Gamma & \cos\Gamma \end{array}} & \\ 0 & & \begin{array}{|cc} \hline 1 & \varepsilon \\ 0 & 1 \end{array} \end{pmatrix}.$$

The functions $e_i(\tau) = D\phi_\tau \cdot e_i(0)$, $i = 1, \ldots, 6$, give us an idea of the variation of the phase space properties in a small neighbourhood of the periodic orbit. Although, instead of them it is more convenient to introduce the *Floquet modes* $\bar{e}_i(\tau)$, $i = 1, \ldots, 6$. Six T-periodic functions that can easily be recovered by $e_i(\tau)$.

The advantage of the Floquet modes is that they can be spanned as a Fourier series and easily stored by their Fourier coefficients. Moreover, we can consider the T-periodic matrix $P(t)$, that has the Floquet modes $\bar{e}_i(\tau)$ as columns. Then, the change of variables $y = P(t)z$, takes the linearisation of equation (1) around a T-periodic orbit, $\dot{y} = A(\tau)y$, to an equation with constant coefficients $\dot{z} = Jz$.

The Floquet modes give us a reference system that is very useful to track, at all time, the relative position between the probes trajectory and the local unstable and stable invariant manifolds to the nominal orbit.

Following (10) we define the first and second Floquet mode taking into account that the rate of escape and approximation, to the Halo orbit, along the unstable and stable manifolds is exponential:

$$\begin{aligned} \bar{e}_1(\tau) &= e_1(\tau)\exp\left(-\tfrac{\tau}{T}\ln\lambda_1\right), \\ \bar{e}_2(\tau) &= e_2(\tau)\exp\left(-\tfrac{\tau}{T}\ln\lambda_2\right). \end{aligned}$$

The third and fourth modes are computed taking into account that the monodromy matrix restricted to the plane generated by the real and imaginary parts of the eigenvectors associated to λ_3 and λ_4 is a rotation of angle Γ:

$$\begin{aligned}\bar{e}_3(\tau) &= \cos\left(-\tfrac{\Gamma\tau}{T}\right) e_3(\tau) - \sin\left(-\tfrac{\Gamma\tau}{T}\right) e_4(\tau),\\ \bar{e}_4(\tau) &= \sin\left(-\tfrac{\Gamma\tau}{T}\right) e_3(\tau) + \cos\left(-\tfrac{\Gamma\tau}{T}\right) e_4(\tau).\end{aligned}$$

Finally, the fifth mode is the vector tangent to the Halo orbit. As it is already periodic we simply put

$$\bar{e}_5(\tau) = e_5(\tau).$$

For the sixth mode we split $e_6(\tau)$ as:

$$e_6(\tau) = \bar{e}_6(\tau) + \epsilon(\tau)\bar{e}_5(\tau),$$

where $\bar{e}_6(\tau)$ is chosen orthogonal to $\bar{e}_5(\tau)$ in the plane spanned by $e_5(\tau)$ and $e_6(\tau)$.

In this new set of coordinates, the dynamics around a Halo orbit is simple. Along the planes generated by $\bar{e}_1(\tau), \bar{e}_2(\tau)$ the trajectory will escape with an exponential rate, along the unstable direction $\bar{e}_1(\tau)$. On the plane generated by $\bar{e}_3(\tau), \bar{e}_4(\tau)$ the dynamics is a rotation around the periodic orbit. Finally, on the plane generated by $\bar{e}_5(\tau), \bar{e}_6(\tau)$ the dynamics is neutral.

3.2. Variation of the linear dynamics

In the previous section we have studied how a trajectory behaves close to a Halo orbit for a fixed sail orientation. Now we want to discuss how small changes on the sail orientation will affect this trajectory.

In section 2.2.1 we have seen that for small changes on the sail orientation, there are no significant changes on the phase space structure. For instance, the Halo - type orbits persist, and the qualitative behaviour around them will be the same.

In the previous section we have described the trajectory of a probe close to a Halo orbit in terms of the Floquet modes. They give us a useful reference system to describe the dynamics close to a periodic orbit. To analyse the effects on the trajectory when we change the sail orientation, it is useful to know how the invariant objects (i.e. periodic orbits, stable and unstable manifolds, ...) vary in this reference system.

As an example we have taken, a Halo orbit ($\phi_\tau(y_0)$) of period $T = 5.389768$ for $\alpha = \delta = 0$, and computed the Floquet modes ($\{\bar{e}_i(\tau)\}_{i=1,\dots,6}$). Then we have computed for different sail orientations ($\delta \in [-0.01 : 0.01]$) the corresponding T-periodic orbit ($\phi_\tau(\hat{y}_0)$) and the corresponding Floquet modes ($\{\hat{\bar{e}}_i(\tau)\}_{i=1,\dots,6}$). We are interested in the relative position of the new periodic orbits and invariant manifolds w.r.t. the nominal orbit $\phi_\tau(y_0)$ and its Floquet modes $\{\bar{e}_i(\tau)\}$.

In Figure 11 we see the relative position of $\phi_{\tau=0}(\hat{y}_0)$ and the eigenvalues $\{\hat{\bar{e}}_i(0)\}$ in the reference system $\{\phi_{\tau=0}(y_0); \bar{e}_{1,\dots,6}(0)\}$.

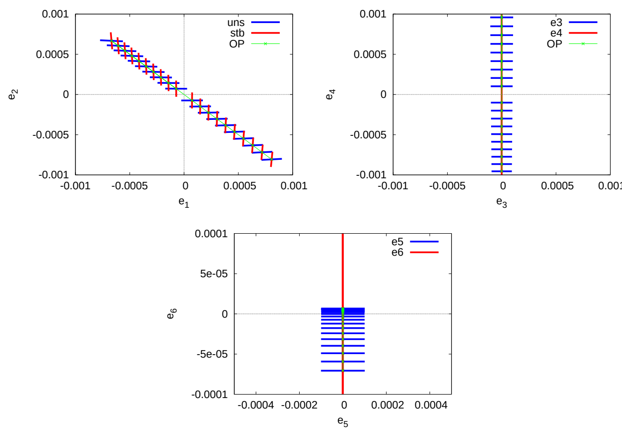

Figure 11: Relative position of the periodic orbit and eigendirections w.r.t. a nominal orbit $\phi_{\tau=0}(y_0)$ in its Floquet bases.

Now let us assume that the probe is close to this T-periodic orbit. In the previous section we saw that the trajectory will escape along the unstable direction and rotate around the periodic orbit on one of the centre projections. Let us discuss what will happen when we change the sail orientation.

As we have seen in Figure 11, when we change the sail orientation, the phase space portrait is shifted: periodic orbits move and the eigendirections are slightly shifted. Now the probe will be close to another periodic orbit, $\phi_\tau(\hat{y}_0)$, and will present the same behaviour as before, but relative to this new periodic orbit, i.e. it will escape along its unstable direction and rotate on its centre projection.

3.3. On the station keeping strategy

To control the instability given by the saddle, we want to find a new sail orientation, such that the new unstable manifold brings the trajectory close to the stable manifold of the nominal periodic orbit, $\phi_\tau(y_0)$. Then we can restore the initial sail orientation and let the natural dynamics act. We can repeat this process over and over to maintain the hyperbolic projection bounded.

To this point we need to understand and quantify how the periodic orbit and their invariant manifolds vary when we change the sail orientation. It is not obvious that we will always be able to find a new periodic orbit, i.e. a new sail orientation, that will bring the trajectory close to the nominal periodic orbit.

In the example shown in Figure 11, the relative position between the periodic orbits that appear when we change the sail orientation and their stable and unstable invariant manifolds is appropriate for this kind of control.

Let us be more concrete, if we are escaping along the unstable manifold, we can change the sail orientation so that the periodic orbit will be shifted with respect to the nominal periodic orbit, as well as the stable and unstable manifolds. As we can see in Figure 11, because the variation of the periodic orbits is along the second and fourth quadrant in the hyperbolic projection, there will be several values for the new sail orientation such that the unstable manifold of the new periodic orbit will bring the trajectory close to the stable manifold of the nominal periodic orbit.

For instance, if the variation of the periodic orbits was in the direction of the stable manifold, it would be impossible to find a change on the sail orientation that would suit us.

In any case, the dynamics on the two centre direction must also be taken into account, as the sequence of changes on the sail orientation can make the centre projection of the trajectory grow.

A more detailed study on the use of the knowledge of the local dynamics around Halo orbits to derive a station keeping strategy is needed. This is actually work in progress.

4. Conclusions

In this paper we discuss the possibility of designing a station keeping strategy for a solar sail around a Halo - type orbit, using dynamical system tools. The idea has been to describe the geometrical structure of the phase space and use it in our favour.

We have considered the Earth - Sun Restricted Three Body Problem for solar sail as a model. We have fixed one of the two sail angles $\alpha = 0$, this means that we only allow vertical variations w.r.t. the Sun - sail. Then we have describer the periodic and quasi-periodic motion around equilibria for different fixed sail orientations ($|\delta| \approx 0$).

Around these equilibrium points the phase space pattern is similar to the RTBP around L_1. There are families of Planar, Vertical and Halo - type orbits, as well as invariant tori.

Finally we have focused on the local dynamics around a Halo - type orbit and discussed how the variation of the sail orientation (δ) affects the probes trajectory. We are now studying the possibility of using the dynamical properties of the system to maintain a solar sail close to these unstable periodic orbit.

Acknowledgements

This work was supported by the CIRIT grant 2009 SGR 67 and the MEC grant MTM2009-09723.

References

[1] J. Bookless and C. McInnes. Control of Lagrange point orbits using solar sail propulsion. In *56th International Astronautical Congress*, October 2005.

[2] J. Carr. *Applications of Centre Manifold Theory*, volume 35 of *Applied Mathematical Series*. Springer-Verlag, New York, 1981.

[3] J. Crawford. Introduction to bifurcation theory. *Reviews of Modern Physics*, 64(4), Oct. 1991.

[4] R. L. Devaney. Reversible diffeomorphisms and flows. *Trans. Amer. Math. Soc.*, 218:89–113, 1976.

[5] A. Farrés and A. Jorba. Dynamical system approach for the station keeping of a solar sail. *The Journal of Astronautical Science*, 58(2):199 – 230, April–June 2008.

[6] A. Farrés and A. Jorba. Solar sail surfing along families of equilibrium points. *Acta Atronautica*, 63:249–257, July–August 2008.

[7] A. Farrés and À. Jorba. On the high order approximation of the centre manifold for ODEs. submited to Discrete and Continuous Serie - B, 2010.

[8] A. Farrés and À. Jorba. Periodic and quasi-periodic motions of a solar sail around the family SL_1 on the Sun - Earth system. submited to Celestial Mechanics, 2010.

[9] G. Gómez, À. Jorba, J. Masdemont, and C. Simó. *Dynamics and Mission Design Near Libration Points - Volume III: Advanced Methods for Collinear Points.*, volume 4 of *World Scientific Monograph Series in Mathematics*. World Scientific, 2001.

[10] G. Gómez, J. Llibre, R. Martínez, and C. Simó. *Dynamics and Mission Design Near Libration Points - Volume I: Fundamentals: The Case of Collinear Libration Points*, volume 2 of *World Scientific Monograph Series in Mathematics*. World Scientific, 2001.

[11] À. Jorba. A methodology for the numerical computation of normal forms, centre manifolds and first integrals of hamiltonian systems. *Experimental Mathematics 8*, pages 155–195, 1999.

[12] À. Jorba and J. Masdemont. Dynamics in the centre manifold of the collinear points of the restricted three body problem. *Physica D 132*, pages 189–213, 1999.

[13] J. Lamb and J. Roberts. Time-reversal symmetry in dynamical systems: a survey. *Phys. D*, 112(1-2):1–39, 1998. Time-reversal symmetry in dynamical systems (Coventry, 1996).

[14] D. Lawrence and S. Piggott. Solar sailing trajectory control for Sub-L1 stationkeeping. *AIAA 2004-5014*, 2004.

[15] M. Lisano. Solar sail transfer trajectory design and station keeping control for missions to Sub-L1 equilibrium region. In *15th AAS/AIAA Space Flight Mechanics Conferece*, Colorado, January 2005. AAS paper 05–219.

[16] M. Macdonald and C. McInnes. A near - term road map for solar sailing. In *55th International Astronautical Congress*, Vancouver, Canada, 2004.

[17] A. McInnes. Strategies for solar sail mission design in the circular restricted three-body problem. Master's thesis, Purdue University, August 2000.

[18] C. McInnes. *Solar Sailing: Technology, Dynamics and Mission Applications*. Springer-Praxis, 1999.

[19] C. McInnes, A. McDonald, J. Simmons, and E. MacDonald. Solar sail parking in restricted three-body system. *Journal of Guidance, Control and Dynamics*, 17(2):399–406, 1994.

[20] L. Rios-Reyes and D. Scheeres. Robust solar sail trajectory control for large pre-launch modelling errors. In *2005 AIAA Guidance, Navigation and Control Conference*, August 2005.

[21] M. B. Sevryuk. *Reversible Systems*, volume 1211 of *Lecture Notes in Mathematics*. Springer-Verlag, Berlin, 1986.

[22] J. Sijbrand. Properties of the centre manifold. *Transactions of the American Mathematical Society*, 289(2), June 1985.

[23] C. Simó. On the analytical and numerical approximation of invariant manifolds. In D. Benest and C. Froeschlé, editors, *Modern methods in celestial mechanics*, pages 285–330. Ed. Frontières, 1990.

[24] V. Szebehely. *Theory of orbits. The restricted problem of three bodies*. Academic Press, 1967.

[25] A. Vanderbauwhede. *Centre Manifolds, Normal Forms and Elementary Bifurcations*, chapter 4, pages 89–169. Dynamics Reported. A Series in Dynamical Systems and their Applications, Vol. 2. John Wiley & Sons Ltd., 1989.

[26] C.-W. L. Yen. Solar sail Geostorm Warning Mission design. In *14th AAS/AIAA Space Flight Mechanics Conference*, Hawaii, February 2004.